Irradiation tests of optical fibers and cables devoted to corium monitoring in case of a severe accident in a nuclear power plant

G. Cheymol, L. Maurin, L. Remy, V. Arounassalame, H. Maskrot, Stéphane Rougeault, V. Dauvois, P. Le Tutour, N. Huot, Y. Ouerdane, et al.

Irradiation tests of optical fibers and cables devoted to corium monitoring in case of severe accident in a Nuclear Power Plant

G. Cheymol, L. Maurin, L. Remy, V. Arounassalame, H. Maskrot, S. Rougeault, V. Dauvois, P. Le Tutour, N. Huot, Y. Ouerdane and P. Ferdinand

***Abstract*—The DISCOMS project considers the use of Optical Fiber Sensing cables embedded into the concrete floor under the reactor vessel for remote monitoring of a severe nuclear accident. This paper focuses on the selection and testing of singlemode optical fibers with limited Radiation Induced Attenuation (RIA). In order to simulate the normal operation period of the reactor, followed by a severe accident, several gamma and mixed (neutron-gamma) irradiations were performed thanks to the CEA Saclay facilities: POSÉÏDON irradiator and ISIS reactor, up to a gamma cumulated dose of about 2 MGy and fast neutrons fluence (E > 1 MeV) of 6×10^{15} n/cm². In comparison with the first gamma test on standalone fibers, a significant increase of the RIA @ 1550 nm appeared during the second test on fibers encapsulated in sensing cables. Molecular hydrogen generated by the cable compounds radiolysis induced an increase of the hydroxyl attenuation broad spectral peak centered at 1380 nm. The radiation-induced OH growth mechanism is confirmed by the comparison of the extended absorption spectral responses of the standalone and encapsulated fibers. A third gamma irradiation run permitted to measure the radiolytic hydrogen production yield of some compounds of a dedicated temperature cable sample. The efficiency of a carbon coating layer over the silica cladding, acting as a barrier against hydrogen diffusion into the optical fiber core, was successfully tested under gamma irradiation as well as in a final test under neutron irradiation.**

***Index Terms*—carbon coating layer, distributed measurement, hydrogen diffusion, gamma, neutron, optical fibers, *rad-hard* optical fiber, radiation effects, radiolysis.**

I. Introduction

In case of severe accident in a Nuclear Power Plant (NPP) leading to both reactor vessel failure and corium spreading, the loss of power supplies will stop the instrumentation, with no way to monitor the status and the evolution of the accident. Especially, the seawater submersion of electrical power supplies caused by the tsunami at Fukushima-Daiichi NPP in March 2011, rapidly lead to a breakdown of most of the instrumentations, leaving the TEPCO operator almost blind, without crucial information coming from the reactor pits, thus making difficult to apply the most appropriate solutions to mitigate the nuclear accident.

Consequently, the so-called RSNR program –dedicated to nuclear security R&D– has been launched in France to improve the mitigation solutions in case of severe accident for Gen II, Gen III, *i.e.* the European Pressurized Reactor (EPR), and for future Gen IV nuclear reactors.

In this framework, the DISCOMS project, which stands for "DIstributed Sensing for COrium Monitoring and Safety", aims at providing innovative solutions not requiring local electrical power supplies, for remote monitoring of such a severe nuclear accident [1].

One of the solutions investigated in the project [2] is based on distributed OFSs (Optical Fiber Sensors) to detect both the onset of the severe accident, the corium pouring on the containment building concrete basemat, and its interaction with the concrete floor until its spreads in the core catcher (in the case of EPR). Such OFSs cables are intended to be embedded into the concrete floor. Temperature and strain profiles can be provided thanks to Brillouin, and/or Raman Distributed Temperature Sensing and Rayleigh Optical Frequency Domain Reflectometry (OFDR), based on the analysis of the

Manuscript received xx.

This project, with reference number ANR-11-RSNR-0007, was carried out within the framework of the RSNR (research on nuclear safety and radiation protection) research program launched after the Fukushima accident, co-funded by the French *Programme d'Investissements d'Avenir* and managed by the ANR (National Research Agency).

G. Cheymol, L. Remy, V. Arounassalame and H. Maskrot are with Den – Service d'Études Analytiques et de Réactivité des Surfaces (SEARS), CEA, Université Paris-Saclay, F-91191, Gif-sur-Yvette, France (+33(0)1.69.08.62.71; e-mail: guy.cheymol@cea.fr).

L. Maurin and S. Rougeault are with Institut LIST, CEA, Université Paris-Saclay, F-91120 Palaiseau, France.

V. Dauvois and P. Le Tutour are with Den – Service du Comportement des Radionucléïdes (SECR), CEA, Université Paris-Saclay, F-91191, Gif-sur-Yvette, France.

N. Huot was with Den – Service d'Exploitation du Réacteur OSiris (SEROS), CEA, Université Paris-Saclay, F-91191, Gif-sur-Yvette, France.

Y. Ouerdane is with Univ Lyon, UJM, CNRS, IOGS, laboratoire Hubert Curien, UMR 5516, 18 rue Prof. B. Lauras, F-42000 Saint-Étienne, France.

P. Ferdinand, previously with Institut LIST, is now with LMP S.A. 49-51 rue du Moulin des Prés, F-75013 Paris, France.

backscattered light in optical fibres. Additionally, such sensing cables can be used as thermal fuses with telecom or photon counting Optical Time Domain Reflectometers (OTDRs) to detect corium vicinity. Detailed description of the measurements considered with these technologies can be found in [1-3].

Usually attenuation in singlemode optical fibers (about 0.2 dB/km at 1.55 µm) is not the main restricting factor for distributed measurements with lengths ranging from hundreds of meters up to several kilometers, but rather the technical limitation of the measurement instrumentation in use. Since ionizing radiations affect their optical transmission properties, it appeared essential for this nuclear application to evaluate the attenuation level induced on long term by these radiations. This paper focuses on the tests conducted in order to expose selected optical fibers and the corresponding sensing cables to irradiation doses expected during the normal operation run of the reactor (up to 60 years for the European Pressurized Reactor), followed by a severe accident occurring at the end of this period, which corresponds to the worst case of radiation dose to be sustained. It is important to notice that one task of the project was precisely to better assess these expected irradiation doses, during normal operation of the reactor [4], and also in case of severe accident. Resistance to temperature rise when the corium approaches the cable, which is of major importance for the severe accident monitoring in order to get measurements from the reactor pit as long as possible, is not in the scope of this work and some complementary information are available in [3]. Tests up to 750°C have been performed, and are discussed in this reference.

Different gamma and mixed neutron/gamma irradiations have been conducted in lab facilities of the CEA research center based in Saclay: POSÉÏDON gamma irradiator and ISIS reactor, up to respectively a gamma dose of about 2 MGy and fast neutrons fluence (E > 1 MeV) equal to 6 x 10^{15} n/cm².

In this paper, we describe the selected fibers and cable, as well as the irradiation conditions for four irradiation tests. Then we present the Radiation Induced Attenuation (RIA) measurements and the corresponding analysis, including the measurements of the radiolytic hydrogen production yield of some compounds of the optical cable.

II. Optical fibers and cables

In our safety related project, even if optical fibers sensing cables are intended to be embedded in the reactor pit concrete basemat, and even if quite short lengths (100 m or less for the sensing part) are considered for corium monitoring, it is necessary to assess the RIA to select the less sensitive fibers in order to be compliant with both the radiation doses to be sustained and the measurement systems optical budgets, in the frame of 60 years of normal operation of the NPP followed by a severe accident.

The behavior of fibers under ionizing radiations, especially γ rays, has been widely studied during the last decades, highlighting the various parameters which impact the RIA levels and kinetics, see [5] for a recent review. The measurement wavelength, which is a critical parameter, is somehow imposed by the available technologies [3]: 1550 nm being the dominating telecom wavelength, for both singlemode fibers and distributed sensing instruments.

The tested Single Mode Fibers (SMFs) are typically 9 µm core diameter, and 125 µm optical cladding diameter, surrounded by a protective coating made of polymer or even metal, leading to an outside fiber diameter typically ranging from 155 µm to 255 µm. In general, optical fiber behavior under ionizing radiations mainly depends on the fiber core composition, where most of the light waves propagate. From previous research works, pure-silica and fluorine-doped cores (both with F-doped cladding) constitute the most radiation-hardened fibers in the domain of dose aimed, up to 100 kGy / 1MGy for steady state irradiation [4], [6], [7].

Selection of the most appropriate OFSs is an important output of the project. So, three different rad-hard optical fibers, named "*a*", "*b*" and "*c*", have been tested under irradiation, as well as a standard Corning™ SMF28 fiber (non *rad-hard*).

Due to the relatively short sensing lengths intended to be used inside the reactor pit in such an application (typ. < 100 m per cable), we stated that the maximum acceptable RIA shall be less than 5 dB at 1550 nm for 100 m, *i.e.* 50 dB/km, with regards to the typical optical budgets of todays distributed measurements systems.

After a first γ irradiation test with a batch of standalone optical fibers, the best 3 *rad-hard* fibers fulfilling these requirements have all been selected, in order to be embedded in 3 different types of sensing cables (distributed temperature and strain measurements cables, plus 'safety' cables) [5] for complementary irradiation tests to evaluate any additional cable impact on the RIA. The irradiation tests were mainly focused on long length temperature sensing cables (a few mm diameters), requiring high irradiator volume capacity.

In addition, a fourth *rad-hard* fiber, named "*d*", incorporating a thin carbon layer between the cladding and the coating, has also been irradiated.

Table 1 sums up the general characteristics of the five tested fibers, and mentions which ones have been inserted in the sensing temperature cable. Cable sections designed with fiber "*i = a, b, c, d*" will be labelled "*Ci*".

TABLE 1.
GENERAL CHARACTERISTICS OF TESTED FIBERS AND CABLES

Fiber	Type of fiber	Associated Cable section
a	*rad-hard*	*Ca*
b	*rad-hard*	*Cb*
c	*rad-hard*	*Cc*
d	*rad-hard* with carbon coating	*Cd*
SMF28	Standard	

III. Irradiations – Experimental test procedure

The irradiations performed in the project aim at testing the fibers and the corresponding cables sections in a configuration which is similar to the aimed environment, or rather in a configuration able to produce the same effects on fibers. We first consider a radiation dose level at the basemat surface in a very conservative configuration, since the reactor concrete basemat will act as a protection against the radiations and will drastically decrease the cumulated doses to be sustained *vs.*

optical cable embedment depth [3].

A. *Irradiation level to withstand*

Two different phases have to be simulated: an operational phase (nominal operation lasting up to 60 years) and an accidental phase with corium spreading out of the reactor vessel. Modeling has shown that the doses are of the same order of magnitude for the operational and for the first 24 h accidental phases, although the dose rates is quite different: in the range of Gy/h for the first, and 20 kGy/h for the second. The RIA depends on the level of cumulative irradiation dose, but also generally, on the dose rate and the complete history in terms of succession of the different dose rates undergone by the optical fiber, the latter being quite complex. In other terms, that is the expected cumulative dose which is first considered below.

On the basis of the information available at the beginning of the project, the nominal configuration –representative of the irradiation level at the top of the concrete basemat, below the reactor vessel– aims to simulate 250 kGy for the operational phase, and at least 450 kGy during the first 24 h of the accident.

Nevertheless, the fine modeling of the γ dose at the concrete surface and assessments made, considering both the operational phase [3] and the first 24 h of the accident, lead us to consider slightly higher dose values: about 1 MGy to a few MGy. It has also been assessed that the operational phase may produce a fast neutrons fluence (E > 1 MeV) up to 10^{15} n/cm² or more on the basemat top surface, leading us to consider irradiation tests in a nuclear reactor core vicinity.

The dose reduction *vs.* the embedment depth has also been considered, it depends on several parameters (concrete type, corium composition…). The evaluation resulted in a reduction of one order of magnitude after the first 40 cm in the concrete floor for both Gen II and Gen III, based on the fact that in the reactor pit, the main damage is the result of 60 years of irradiation during normal operation [3].

B. *Irradiation facilities*

γ irradiations have been carried out in the POSÉÏDON industrial pool type irradiator of the Applied Radiation Laboratory (LABRA) [8] based in Saclay. In the associated casemate, 2 source planes produce about 10,000 TBq (300,000 Ci), for a maximum dose rate of 6 kGy/h, homogeneous (± 10%) between the source planes in a volume of approximate dimensions: 1 m x 0.6 m x 0.4 m (Fig. 1). The irradiation runs were performed at room temperature (RT), 20°C to 30°C, or at 80°C by using an adapted oven located in the irradiator casemate.

Neutron irradiations were carried out in the ISIS research reactor [9] (which is now shut down), mainly dedicated to education and training, with a nominal power of 640 kW. Optical fibers samples were placed in small capsules in the vicinity of the reactor core. Fast neutrons (E > 1 MeV) flux was 2.8 x 10^{11} n/cm²/s. Thermal neutrons flux was 2.4 x 10^{12} n/cm²/s, superposed with an associated 50 kGy/h γ dose rate. The temperature during the irradiation was about 40°C.

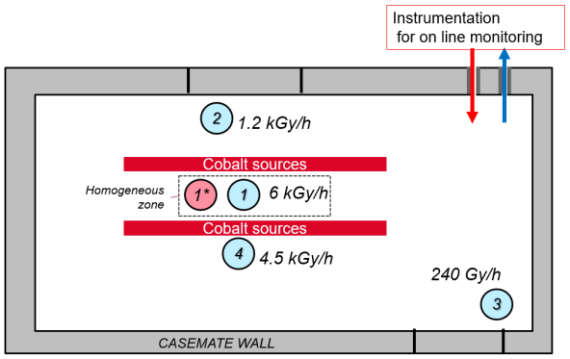

Fig. 1. Diagram of the POSÉÏDON casemate with positions used in the project and associated dose rates. Configuration 1* differs from configuration 1 by a higher temperature (about 80°C instead of room temperature).

C. *Four successive irradiation tests*

1) *Irradiation 1: γ irradiation of 100 m long fibers*

The 100 m long fibers were wound on a 15 cm diameter strand and connected thanks to a feedthrough, to an instrumentation located outside the casemate for online monitoring. The optical fibers were tested in 4 configurations, with different dose rates or temperatures. In the nominal configuration, fibers were first in position ② (see Fig. 1) during 215 h, then moved to position ① for the next 113 h (this configuration being named "② to ①"). A total fluence 5 times lower was tested with the configuration "③ to ②".

The maximum fluence achieved during the irradiation test was performed by leaving fibers all the time in the position ①, or ①*, which also permitted to assess the impact of increased temperature.

RIA on segments of fibers approaching the inter-source zone (about 2 m not shielded) is neglected, since the flux quickly decreases away from the sources.

Table 2 gives the temperature, dose rate, cumulated dose for each phase of the irradiation 1, for the 4 configurations.

TABLE 2
IRRADIATION 1: γ IRRADIATION OF FIBERS,
DOSE AND DOSE RATE IN 4 CONFIGURATIONS

Config.	Temp.	Operational Phase (215 h): dose *dose rate*	Accident (113 h): dose *dose rate*	Total (328 h): cumulated dose
② to ①	22°C	250 kGy *1.2 kGy/h*	650 kGy *5.7 kGy/h*	900 kGy
③ to ②	22°C	49 kGy *230 Gy/h*	131 kGy *1.2 kGy/h*	180 kGy
①	22°C	1.2 MGy 5.7 *kGy/h*	650 kGy *5.7 kGy/h*	1.9 MGy
①*	80°C	1.2 MGy 5.7 kGy/h	650 kGy 5.7 kGy/h	1.9 MGy

2) *Irradiation 2: γ irradiation of 100 m long optical cables*

Optical sensing cables "*Ca*", "*Cb*" and "*Cc*" equipped with *rad-hard* selected optical fibers have been irradiated. This time, the 100 m long cables give a much more voluminous strand, typically 40 cm diameter with a section of 5 cm or greater. Thankfully, the POSEÏDON irradiator is well adapted to this run since it presents a relatively large irradiation zone with an homogeneous dose rate spatial distribution.

Here again, the cables were connected to a remote distributed instrumentation located outside the casemate for online monitoring. We kept the coiled cables in the same position during the 300 h irradiation time, since it would have been much more difficult (compared to the previous test) to move the coils from one position to another.

We took care to avoid differences in cumulated dose, since one strand may sometimes shade the adjacent one. That is why we coiled 100 m lengths of the three different cables of interest on one single strand. So that, the mean dose rates received by each 100 m cable were very similar: about 5 kGy/h, even if some parts undergone 15% less while others 15% more. The irradiation lasted 303 h, resulting in a cumulated dose of 1.5 MGy.

It is mainly the positions ① and ①* that were used. However, one cable was in the position ②, with a dose rate of 1.05 kGy/h resulting in a 320 kGy cumulated dose.

3) Irradiation 3: γ irradiation of short length of optical fibers and cable

Short lengths of optical fibers cables and bulbs with various components of the temperature cable, have been irradiated in the position ④, but without online measurement. The dose rate was set to 4.5 kGy/h during 400 h, leading to a cumulated dose of ~ 1.8 MGy.

4) Irradiation 4: neutrons + γ irradiation of short optical fiber lengths

Short lengths of optical fibers have been irradiated in the vicinity of the ISIS reactor core, without online measurement. The fibers were wound in several strands of diameters ranging from 3 cm to 4 cm.

The power of the reactor was set to 640 kW, the irradiation lasted 6 hours. Dose rate and cumulated dose are displayed on Table 3.

TABLE 3
TEST 4: n + γ IRRADIATION OF OPTICAL FIBERS

	DOSE RATE	DOSE
Fast neutrons	2.8 x 10^{11} n/cm²/s	6 x 10^{15} n/cm²
Thermal neutrons	2.4 x 10^{12} n/cm²/s	5.2 x 10^{16} n/cm²
γ	50 kGy/h	300 kGy

D. RIA measurement setup

During the γ irradiation test 1 and test 2, the RIA was continuously monitored. Fig. 2 shows the measurement set-up.

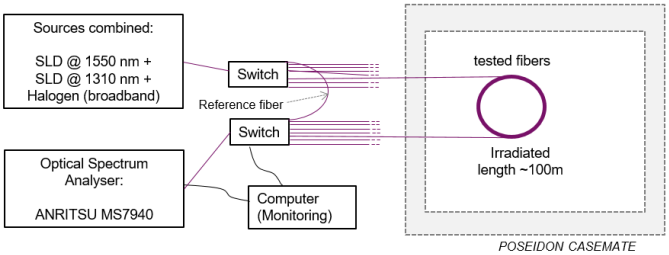

Fig. 2. On-line measurement set-up diagram.

Even if the 1550 nm nominal wavelength was especially considered, it was also interesting to assess the RIA on a larger spectral range. On that purpose, the beams of two SLED, centred at 1550 nm and 1310 nm, and a large spectrum halogen source were combined with optical fiber couplers. In order to avoid any photobleaching, as far as possible, the total power injected in the fibers under test was in the range of 1 µW.

IV. RESULTS AND ANALYSIS OF TEST 1: γ IRRADIATION OF THE *RAD-HARD* SINGLEMODE OPTICAL FIBERS

A. Results

The various configurations have been described in section III with a summary in Table 2.

For all considered optical fibers, the RIA increases during the irradiation, faster when the dose rate is higher, as depicted on graph related to configuration ② to ① (Fig. 3).

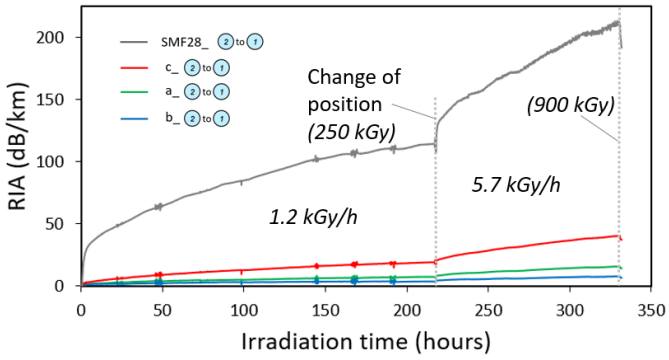

Fig. 3. RIA@1550 nm *vs.* time for fibers *a*, *b*, *c* and SMF 28 during irradiation 1 / configuration "②to①". The dose rate is 1.2 kGy/h before the change of position, and 5.7 kGy/h after.

The RIA, at 1550 nm, at the end of irradiation for *rad-hard* fibers *a*, *b* and *c* in configuration ② to ①, are 14 dB/km, 7 dB/km and 34 dB/km respectively. In the configuration ③ to ②, with five times lower dose rate, the RIA is approximatively divided by a factor of 2. Fig. 4 shows the difference in RIA for the *rad-hard* fibers when they are irradiated at either 22°C or 80°C. Except for the first 30 hours of the irradiation of fiber c, the RIA decreases when the temperature increases, as already reported, *e.g.* in [10]. This trend is favorable in the perspective of still higher temperature when the corium approaches the fiber. The decrease of RIA with temperature appears here even lower when the RIA is weak.

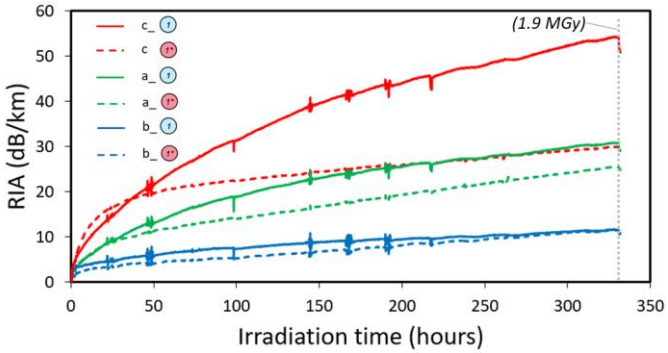

Fig. 4. RIA@1550 nm vs. *time for fibers a, b, c during irradiation 1 in configuration ① (22°C) and ①* (80°C). The dose rate is 5.7 kGy.*

Noised parts on the graphs of Fig. 3 and Fig. 4 were attributed to the unexpected sun illumination of the bench outside the irradiator.

The measurements on a larger spectrum show that RIA decreases when λ decreases towards 1 µm. The ratio of RIA at 1550 nm over its value at 1310 nm is about 1.5 with irradiations conducted at 22°C and higher (greater than 2) with irradiations performed at 80°C (Fig. 5).

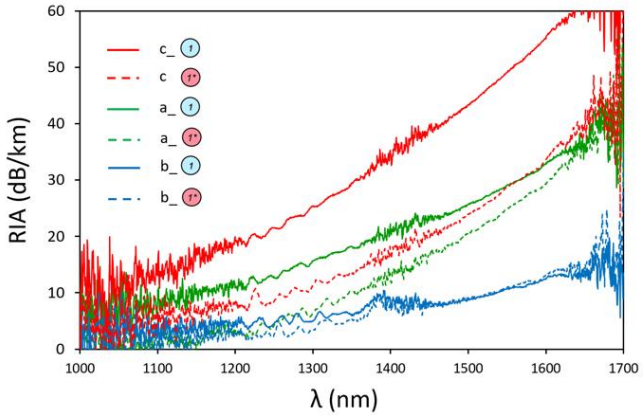

Fig. 5 : RIA spectrum for fibers *a*, *b*, *c* at the end of irradiation 1 in configuration ① (22°C) and ①* (80°C).

B. *Variation of RIA with the dose rate - Accelerated tests*

As mentioned above, in the configurations ② to ①, and ③ to ②, the first part of the test is a highly accelerated test. The representativity of that test must be interrogated, raising the question of the RIA variation *vs.* the dose rate.

The tests conducted at different dose rates permitted to assess how the RIA depends on dose rate when the latter varies in a ratio of 25. Depending on the fiber, the RIA may change by a factor of 2 or show little variations with the dose rate, like for fiber *c* (Fig. 6), for which RIA varies roughly according to the following law on a large scale: $RIA = A \times \sqrt{D}$. This reinforces our approach of taking into account first the cumulated dose, even if the minimum tested dose rate is still much higher than the expected one during the operational phase. The literature generally reports that RIA is reduced when the dose rate decreases, as we observed also on fibers *a* and *b*. Then we believe that the RIA expected for the operational phase is well assessed (fiber *c*) or rather overestimated (fibers *a* and *b*).

This first test confirmed that some *rad-hard* optical fibers have much less RIA than standard commercial Ge-doped fiber, in the range of 50 dB/km or less (down to 10 dB/km), at 1550 nm and a cumulated dose of 1 MGy or greater.

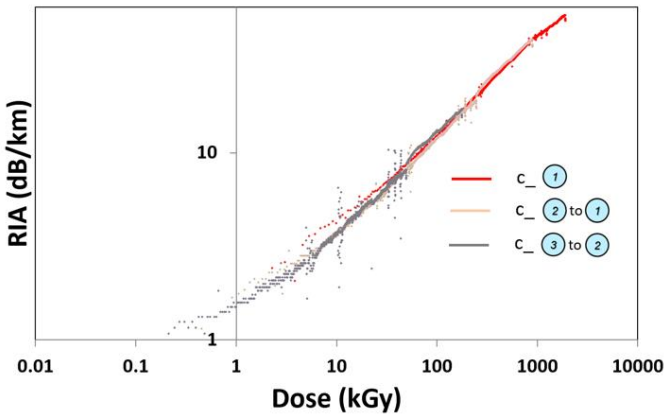

Fig. 6. Evolution of fiber *c* RIA *vs.* cumulated dose (logarithmic scales) for the 3 configurations : ①, ② to ①, and ③ to ②. The RIA varies slightly with the configuration, *i.e.* with the dose rate. As a first approach, this evolution can be fitted by using a least squares method : $RIA = A \times \sqrt{D}$.

V. Results and Analysis of Test 2: γ Irradiation of Optical Sensing Cables

A. *RIA of fibers in cable at 1550 nm*

The selected *rad-hard* optical fibers have been inserted in sensing cables and irradiated in the POSÉÏDON irradiator. We focus below on the tests of the temperature sensing cables in configurations ① and ①* (Fig. 1). For comparison, we also irradiated the same fibers, conditioned in the same way (*i.e.* not inserted into cable, but standalone), like the previous test based on configuration ①.

The RIA levels of the optical fibers inserted into cables are significantly higher than those of the same standalone fibers, as depicted on Fig. 7 for fiber *a*.

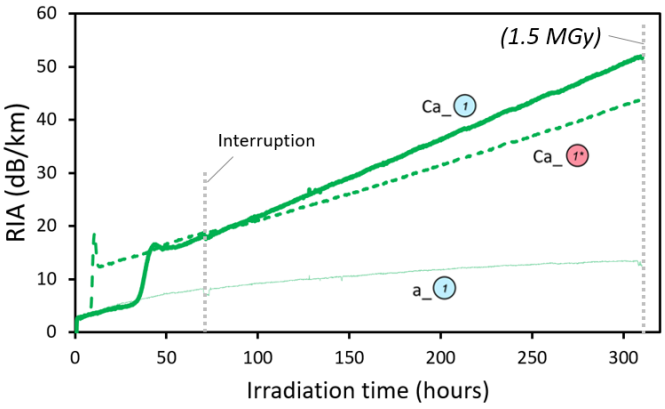

Fig. 7. Irradiation 2, RIA@1550 nm *vs.* time for fiber *a* in position ① (see Fig. 1) at 30°C, and cables *Ca* at 30°C (position ①) and at 80°C (position ①*). The dose rate is about 5 kGy/h.. After 35 h, the graph of RIA for the cable at 30°C separates from the graph of RIA of the fiber in same position and temperature. The irradiation was interrupted[1] during 3 hours, from 70 h to 73h.

For the three optical sensing cables (Fig. 8):

- The RIA at the end of irradiation phase is greater for fibers embedded into cable than for standalone fibers,
- The RIA does not exhibit any tendency to saturation,

[1] Due to a false fire alarm in the facility.

- After a while, the graph of RIA *vs*. time (*i.e. vs.* dose) for the cable at room temperature (position ①) separates from the graph of RIA of the optical fiber at the same position. This event occurs after a period of time which depends on the fiber,
- This event can give rise to a jump: peak of RIA (rapid increase, then decrease). This peak is higher at 80°C than at 30°C, and it appeared to be higher at 1310 nm than at 1550 nm.

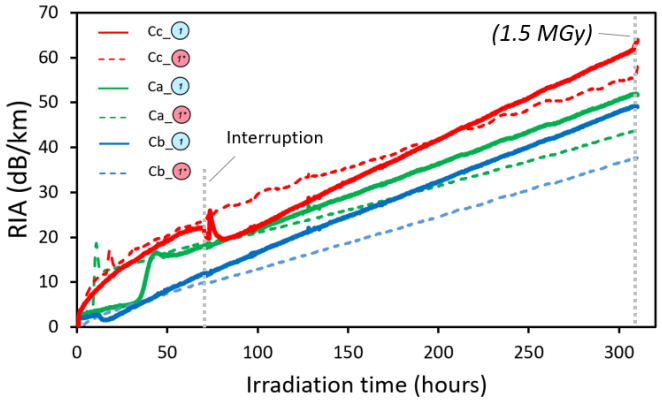

Fig. 8. RIA@1550 nm *vs.* time for cables *Ca*, *Cb* and *Cc*, during irradiation 2, in both configurations ① (30°C) and ①* (80°C). The dose rate is about 5 kGy.

Fig. 8 shows that there is less difference between RIA of various fibers in cable than observed for standalone fibers (see Fig. 4). It comes with the fact that fiber *c* and cable *Cc* present nearly the same RIA at the end of the irradiation (Fig. 9).

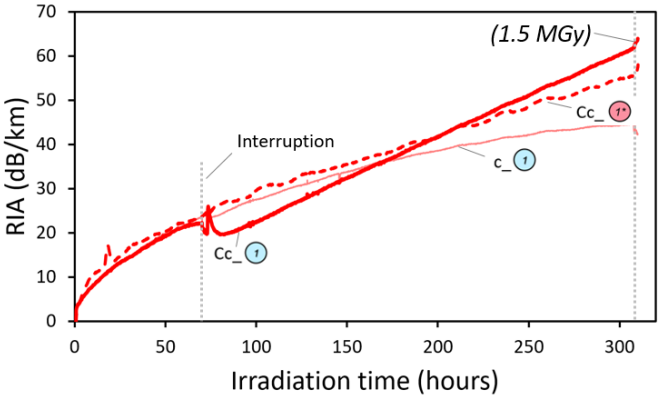

Fig. 9. Irradiation 2, RIA @ 1550 nm *vs.* time for fiber *c* in position ①, at 30°C, and cables *Cc* at 30°C (position ①) and in oven at 80°C (position ①*).

We can also notice that the RIA of the standalone optical fiber *a* located at room temperature is lower in irradiation 2 (Fig. 7) than in irradiation 1 (Fig. 4), for the same dose. At 1.5 MGy: about 25 dB/km for test 1 and about 12 dB/km for test 2. That is not the case for fibers *b* and *c*. New batches of fibers were ordered after the selection consecutive to irradiation 1 in order to be embedded in cables. Then, fibers *a*, *b and c* for irradiations 1 and irradiation 2 are not from the same batches. We did not further test the batch-to-batch variation.

Also, the cable *Ca*, irradiated at room temperature in position ② with about 5 times lower dose rate (about 1 kGy/h instead of 5 kGy/h) –and then with also 5 times lower accumulated dose– was 2.5 times less affected than the cable *Ca* irradiated at room temperature in position ①.

B. RIA on larger spectrum – OH peak

The graphs of RIA spectrum on a large spectrum range enlighten the difference between RIA in standalone fibers and RIA in fibers inserted in cables. The increase of the RIA at 1550 nm is due to the large attenuation peak centred at 1380 nm (Fig. 10), which reveals the presence of hydroxyl groups in the fiber core.

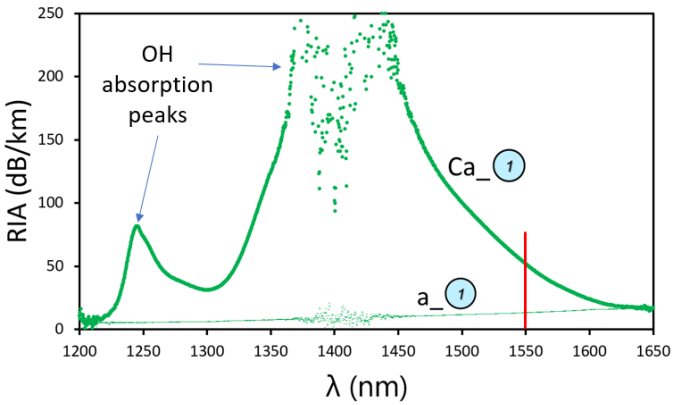

Fig. 10. RIA spectrum for fiber *a* and cable *Ca* at the end of irradiation 2 (cumulated dose: 1.5 MGy), in position ① (30°C/ 5 kGy/h). The top of the peak centered at 1380 nm is not accessible since its level is very high (out of our measurement's range). Actually, 1245 nm is also an absorption peak related to hydrogen, which probably contributes to that secondary peak.

Such OH peak is likely to be generated by the production of hydrogen *via* radiolysis of polymer compounds of cables [11]; the hydrogen then diffuses towards the fiber core and induces the creation of hydroxyl groups. Such phenomenon was reported [12] on standalone polymer coated fibers with irradiation in reactor. Except under this harsh mixed gamma + neutron environment, the increase of the OH peak is reported - on standalone fibers – with H_2 loading prior to gamma irradiation [13]. But we did not find any report dealing with a significant increase in the OH peak without the addition of external hydrogen at a similar gamma dose level (in the MGy range) as we obtained in our experiments.

Without irradiation, the increase of the OH peak is also reported at high temperature [14], and [15] mentioned that OH growth due to H_2 presence has not been observed at room temperature[2], while [14] pointed out the irreversibility of the reaction.

In the literature, the increase of the OH peak is either a drawback for applications in the IR domain ([14], [16]) like for DISCOMS project, or a side effect of a researched passivation of NBOHC defects (resulting from the breaking of a Si-O-Si bond) in the visible range ([17], [18], [19]) in order to increase the fiber transmission in that domain. The related reaction is as follows (1):

$$SiO\bullet + H\bullet \rightleftharpoons SiOH \qquad (1)$$

[2] Except for fibers highly doped with Phosphorus.

Fig. 11 illustrates well the described effect: it displays the attenuation graph over a spectral range including both the visible and the near-IR domains, obtained four months after the end of the irradiation, on fiber *a* and cable *Ca*. The attenuation of fibers was measured thanks to a strongly attenuated Supercontinuum source, and an ANDO™ 6315 OSA. The fiber in cable shows a high OH peak, but no peak in the visible range, whereas the standalone fiber has no OH peak and highlights a significant signal in the visible range. The 2 eV absorption band, at high ionizing dose (MGy range), is mainly attributed to the NBOHC [19], [20].

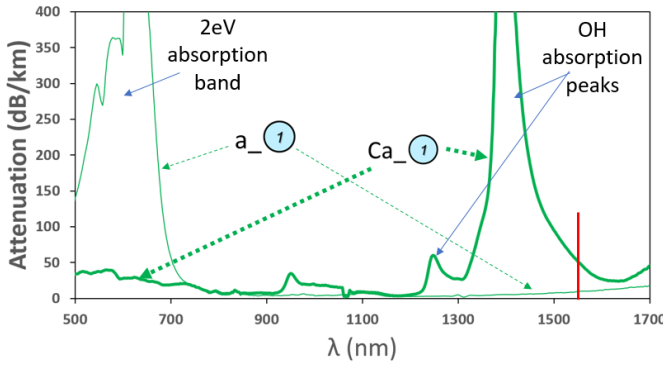

Fig. 11 RIA spectrum for fiber *a* and cable *Ca* four months after the end of irradiation 2 (cumulated dose: 1.5 MGy), in position 1 (30°C / 5 kGy/h). Measurement is performed with higher dynamics than in Fig. 10, but the top of the peak centered at 1380 nm is still not accessible, neither the top of the peak in the 2eV absorption band.

The absence of H_2-induced absorption peak at 1132 nm and 1083 nm (Fig. 11) permits to conclude that H_2 is no more present in the fiber core. The absorption peak at 1245 nm is then only related to OH groups. [21] reported the attenuations in dB/km/ppm for the wavelength of the major absorption peak of SiOH (2.7 µm), for the different harmonics and their combinations with the silica network vibration modes. We can then deduce the amount of hydroxyl groups in the irradiated fiber core to be about: 20 ppm. And also, [21] permits - thanks to the peak at 1245 nm - to assess the absorption level at 1380 nm (when our measurement cannot directly provide this information). It is estimated to 1.3 dB/m by applying a factor of 23 to the attenuation obtained at 1245 nm, which is accessible (60 dB/km as reported on Fig. 11).

Like NBOHC, the well-known SiE' point defect in pure silica, is likely to react with hydrogen through the simplified reaction:

$$Si\bullet + H\bullet \rightleftharpoons SiH \qquad (2)$$

SiH may also appear together with SiOH when a silica bond is broken, in particular under irradiation, in presence of hydrogen [18, 22]:

$$Si\bullet + SiO\bullet + H2 \rightarrow SiOH + SiH \qquad (3)$$

The absorption signature of SiH is not present in our RIA spectral response, except during the jumps (events with rapid increase of RIA and then decrease) described earlier, when the graph of RIA *vs*. time for the fiber embedded in cable separates from the same graph of the standalone fiber (events well distinguishable on Fig. 7). Fig. 12 displays the RIA spectra for fiber in cable *Ca* in position 1* (80°C/ 5 kGy/h) at 6 different times during the jump of RIA *i.e.* from the time of irradiation 8 h to the time 13h. The noticeable decrease of the RIA @ 1550 nm after reaching the top of the peak can be clearly attributed to the dynamics of the SiH peak. This peak increases and then disappears at the end of the short period observed. However, the newly created OH peak centered at 1380 nm extends up to 1550 nm, resulting in a significant permanent increase in RIA compared to what it was before the event. On the left side of the OH peak, and especially at 1310 nm, the RIA increases and then decreases without it being possible to associate this phenomenon with a well located peak.

The difference in presence of signatures due to SiH and SiOH may be due to different dynamics in the creation of SiOH and SiH centers, with the chemical equilibrium of reaction (1) being much more shifted to the right than the one related to equation (2). The whole dynamics is not well understood yet.

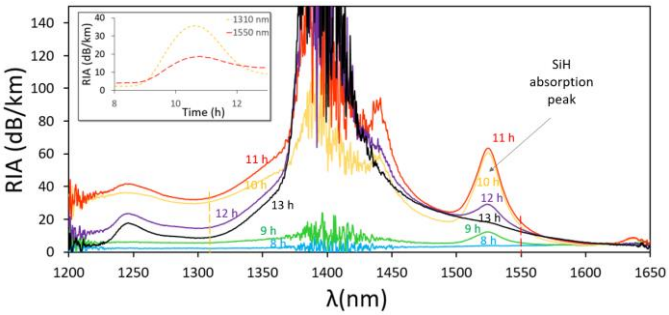

Fig. 12. RIA spectra for fiber in cable *Ca* in position 1* (80°C/ 5 kGy/h) at different times during the jump of RIA *i.e.* from the time of irradiation 8 h to the time 13h (see Fig. 7). In the inset: RIA versus time @ 1310 nm and 1550 nm. The top of the jump is at 11 h approximately.

Also, we could make the assumption that the events with rapid increase of RIA correspond to the time when hydrogen reaches the fiber core after its diffusion from outside. Indeed, before that time, the RIA of the fiber in cable is likely to be the same as the one of the standalone fiber. After that time, when hydrogen is significantly present in the fiber core, RIA differences between fiber in cable and standalone fiber are expected to appear. This hypothesis is consistent with the fact that the event occurs earlier with cable heated at 80°C than with the cable at room temperature, since the diffusion rate increases with temperature [23], [24]. But the different times of appearance and the different peak heights for *rad-hard* fibers with only a few slight differences in the coating and embedded in the same sensing cable could indicate that the whole dynamic of the events is not only related to the simple diffusion of hydrogen. All these phenomena are not trivial to explain and deserve more attention in the future.

VI. Results and Analysis of Test 3: γ Irradiation of Cables and Carbon Coated Optical Fiber Parts

A. *Irradiation of short lengths of cable*

Avoiding or reducing the amount of hydrogen diffusing towards the fiber core is of scientific interest even if the RIA observed with fiber into cables remains acceptable for this

project, mainly because its embedment in the concrete will significantly decrease the dose received by the fibers [3]. To that end, we have tested a cable equipped with a carbon coated fiber. Such a thin carbon layer is known to protect the silica-based fibers from external hydrogen diffusion [25]. Metallic coating (Al, Cu, Au) remain another option to prevent or slow down hydrogen diffusion into the core, but metallic coatings are less hermetic and generate stresses on the fiber, in particular due to the differential thermal expansion with the silica fiber. We rather try to avoid such stresses in optical fiber sensing.

The tested cable incorporating the carbon coated fiber was not made according to standard manufacturing procedure: the original optical fiber was replaced off-line in the temperature cable by a rad-hard carbon coated fiber "*d*", thus giving cable "*Cd*" (see Table 1). Then, 3.4 m length of this cable *Cd* was irradiated, as well as the same lengths of cables *Ca*, *Cb*, and *Cc* placed in position ④ inside the POSÉÏDON irradiator (see Fig. 1), at the dose rate of 4.5 kGy/h during 401 hours, leading to a cumulated dose of 1.8 MGy. There was no on-line monitoring. The focus on the OH peak, with potentially high expected RIA level, is compatible with the short fiber lengths tested.

Following the irradiation phase, the attenuation of fibers inserted into cables was measured thanks to a strongly attenuated Supercontinuum source, and the same ANRITSU™ OSA as used in previous on-line experiments. The sample tested were pigtailed and the attenuation introduced by this assembly was measured. The lack of repeatability in the losses of optical fiber connections and of the splicing to the pigtails prevents to make reliable absolute measurements of the attenuation. Fig. 13 presents the difference with the attenuation measured at 1200 nm on the assembly including the irradiated sample to test. That implied a vertical translation of the curves to cancel the attenuation at 1200 nm. At that wavelength, the RIA should be very low on such short lengths. Therefore, negative values on the graphs are not expected. These graphs show the absence of any OH optical signature for the irradiated cable with the carbon coated fiber, which demonstrates the efficiency of such carbon layer for the intended purpose.

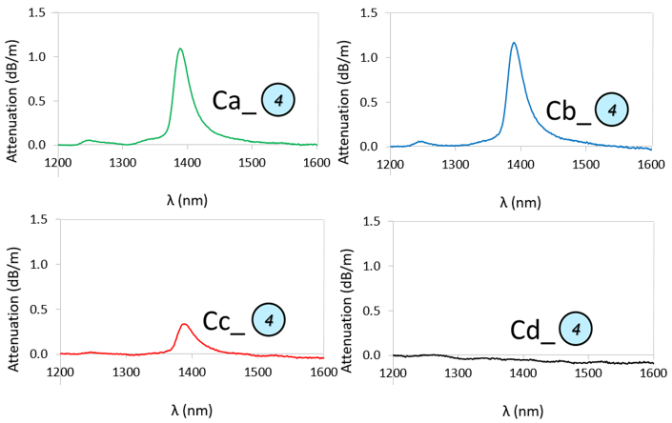

Fig. 13. Spectrum of the difference with the attenuation measured at 1200 nm for cables *Ca*, *Cb*, *Cc*, *Cd* after irradiation 3, in position ④ (22°C; 4.5 kGy/h; 1.8 MGy).

The OH peak (about 1 dB/m) is similar to the one observed during the irradiation 2, except for Cable *Cc*; the reason for this weaker peak is not explained yet.

We also irradiated short lengths of optical fibers *a*, *b*, *c* and *d*, sealed in a small and virgin (*i.e.*: without any polymer traces) metallic tube (same as the ones used in some strain sensing cables [3]), previously dried during 4 hours at 150°C, and then we measured the attenuation spectra at the end of the irradiation. There was no trace of any OH peak for all optical fibers, which also demonstrates that the radiolysis of the polymer coating around the fiber does not produce, in these conditions of irradiation, enough hydrogen to induce an OH signal, even if the produced molecular or atomic hydrogen is kept in the fiber vicinity.

B. Production of hydrogen of different compounds of cables – Radiolytic hydrogen production yield

To complete the study of induced attenuations, additional measurements were carried out on specific components of the temperature sensing cable, in order to study the formation of volatile compounds, and in particular H_2 dihydrogen, during the irradiation 3.

These materials were kept in sealed glass bulbs and have been irradiated. In particular, the gel in contact with the optical fiber, used in the temperature cable to improve its efficiency for temperature measurements, was tested, and also the overall cable, mainly made of one surrounding polymer material. For each material, 2 bulbs approximately 20 cm long were used with reconstituted air (including krypton as tracer). Two bulbs with only reconstituted air have been added for reference. The irradiated bulbs are shown on Fig. 14.

Fig. 14. Different bulbs with various components of the temperature sensing cable inside, after irradiation 3 at a dose of 1.8 MGy.

At the end of the irradiation, the gaseous mixture in each ampoule was analysed by direct injection mass spectrometry and magnetic sector, to obtain both characterization and quantification of all species. The formation of hydrogen, expressed in number of moles per unit length of fiber, or cable, is recorded in Table 3.

TABLE 3
HYDROGEN PRODUCTION AT 1.8 MGy IRRADIATION DOSE

Component	Bulb #	Hydrogen produced (mol_H_2/m)
Coated fiber	1	8.6×10^{-7}
	2	9.8×10^{-7}
Gel	3	6.6×10^{-4}
	4	7.2×10^{-4}
Overall cable	7	4.2×10^{-3}
	8	5.4×10^{-3}

The overall optical cable and its surrounding polymer material produce the major part of hydrogen while irradiated. Dividing this production by the mass of each component permits to calculate the radiolytic hydrogen production yield. The higher value is due to the gel, with a yield of about 2×10^{-7} mol/J for an irradiated sample at a dose of 1.8 MGy.

VII. n + γ IRRADIATION OF SHORT FIBER LENGTHS

Finally, the efficiency of the carbon coating layer was also investigated under neutron irradiation, up to a fast neutrons fluence of 6×10^{15} n/cm² (see § II. C. 4). The main objective of this experiment was to provide information about the RIA resulting from the neutron fluence during the operational phase.

About 10 m long optical fibers were irradiated in the vicinity of the ISIS reactor core, for *post-mortem* measurement. The fibers were wound in several strands of diameters ranging from 3 cm to 4 cm, and inserted into sealed vinyl plastics sachets. The whole set of four fibers *a*, *b*, *c* and *d* was tested. Fibers *c* and *d* were also investigated when soaked with the gel used in temperature sensing cables. The sachets were then inserted in aluminium capsules.

Following the irradiation, the spectral attenuations of these optical fibers were evaluated with focus on the OH peak like in the previous experiment (see § VI A). Corresponding graphs of attenuation are displayed on Fig. 15.

The first point to notice is that, in this experiment, even for standalone fibers without any compound of cable surrounding gel, we observe an OH signal, on the contrary to what happened on previous gamma irradiations. The outbreak of an OH peak could result, like in [12], from the fact that the irradiation flux is much higher than in previous tests. The large amount of hydrogen produced by the radiolysis of water all around the capsules in the pool, associated with the large capability of hydrogen diffusion, may also have contributed to the presence of hydrogen in the fiber core, even for standalone fibers. Also, the vinyl plastics sachets may have contributed to the production of hydrogen. We note that the presence of gel around the fiber *c* does not change much the amplitude of the OH peak in comparison with fiber *c* without gel.

The other point to notice is, once again, the absence of large OH peak in the carbon coated fiber *d*, soaked with gel or not, which confirms the efficiency of such carbon layer to protect against the diffusion of hydrogen towards the core of the fiber, even in presence of neutron radiation.

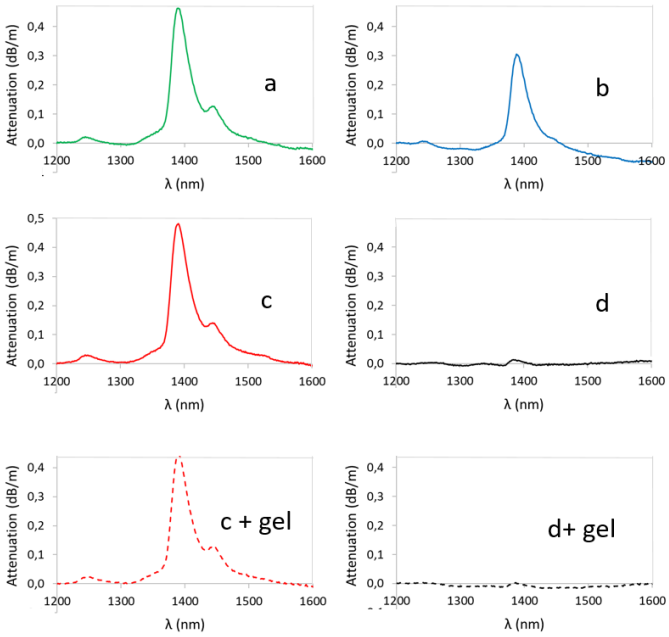

Fig. 15. Spectrum of the difference with the attenuation measured at 1200 nm for fibers alone, or soaked with gel after irradiation in the vicinity of the ISIS reactor core.

The associated gamma dose during the irradiation in the ISIS reactor was about 300 kGy, the same dose as received by the fiber in cable set at the position ② during the second gamma irradiation (see § III. C. 2), and with the same amplitude of the OH peak: about 0.4 dB/m. This result tends to confirm that a fast neutrons fluence of 6×10^{15} n/cm² does not produce a significant RIA increase when associated with a gamma dose of some hundreds of kGy. That is in good agreement with the fact that the secondary ionization effects induced by such neutrons fluence is equivalent to a gamma dose from 1 kGy to a few kGy. Indeed, the secondary ionization effects induced by a fast neutrons fluence from 10^{12} n/cm² to a few 10^{12} n/cm² are equivalent to a gamma dose of 1 Gy [26], [27]. Our result is also in agreement with results of [28].

VIII. CONCLUSION

We have presented and analysed various RIA measurements of standalone *rad-hard* optical fibers and of fibers embedded in cables, showing a significant increase of the RIA @ 1550 nm for fibers in cable. This increase is due to molecular hydrogen generated by the compounds' radiolysis of the cable.

Thanks to different tests conducted, we have been able to recommend the better *rad-hard* optical fiber for the aimed application, compliant with 60 years of normal operation of the NPP followed by a severe accident, and compliant with an installation respectively at minimum 30 cm and 5 cm below the surface of the concrete basemat for Gen II and Gen III reactors.

An optical fiber with carbon coating layer should therefore be systematically preferred for such application, or/and either any other means to protect the fiber core from the diffusion of hydrogen and its effects on attenuation. However, the long-term efficiency of the carbon coating under ionizing radiations shall be further investigated.

REFERENCES

[1] P. Ferdinand, S. Magne, and G. Laffont, "Optical Fiber Sensors to improve the safety of Nuclear Power Plants," Asia Pacific Optical Sensors, APOS2013, Wuhan, China, 17th-21st Oct. 2013.

[2] P. Ferdinand *et al*, "DISCOMS: DIstributed Sensing for COrium Monitoring and Safety," CANSMART, Vancouver, BC, Canada, 15-17 July 2015. https://hal-cea.archives-ouvertes.fr/cea-02151741

[3] L.Maurin et al., "Remote monitoring of Molten Core-Concrete Interaction experiment with Optical Fibre Sensors & perspectives for severe nuclear accident monitoring – DISCOMS project," 6th international conference on Advancements in Nuclear Instrumentation Measurement Methods and their Applications, ANIMMA 2019, 17-21 June 2019, Portorož, Slovenia.

[4] M. Brovchenko, I. Duhamel, and B. Dechenaux, "Neutron-gamma flux and dose calculations for feasibility study of DISCOMS instrumentation in case of severe accident in a GEN 3 reactor." EPJ Web of Conferences 153, 07030 (2017) - ICRS-13 & RPSD-2016. 25 Sept. 2017. https://doi.org/10.1051/epjconf/201715307030.

[5] S. Girard *et al.*, "Recent advances in radiation-hardened fiber-based technologies for space applications", Journal of Optics, vol 20, no. 9, Aug. 2018, Art. no. 093001.

[6] T. Wijnands, L. K. De Jonge, J. Kuhnhenn, S. K. Hoeffgen, and U. Weinand, "Optical absorption in commercial single mode optical fibers in a high energy physics radiation field," IEEE Trans. Nucl. Sci., vol. 55, no. 4, pp. 2216–2222, Aug. 2008.

[7] X. Phéron, S. Girard, A. Boukenter, B. Brichard, S. Delepine-Lesoille, J. Bertrand, and Y. Ouerdane, "High -ray dose radiation effects on the performances of Brillouin scattering based optical fiber sensors," Opt. Exp., vol. 20, pp. 26978–26985, 2012.

[8] http://www-centre-saclay.cea.fr/fr/Le-Labra-une-plateforme-d-irradiation-au-service-des-industriels-et-des-chercheurs

[9] F. Foulon, B. Lescop, and X. Lohleber, "Development of education and training programs using ISIS research reactor". Joint IGORR 2013 & IAEA Technology Meeting, Korea, 13-18 Oct 2013.

[10] J. Kuhnhenn, S. K. Hoffgen, and U. Weinand, "Quality Assurance for Irradiation Tests of Optical Fibers: Uncertainty and Reproducibility", IEEE Trans. Nucl. Science, vol. 56, no. 4, pp.2160-2166, August 2009.

[11] M. Ferry *et al*, "Ionizing radiation effects in polymers," Reference Module in Materials Science and Materials Engineering, Elsevier (2016).

[12] B. Brichard, B. Borgermans, A.F. Fernandez, K. Lammens, M. Decreton. "Radiation effect in silica optical fibre exposed to intense mixed neutron gamma radiation field", IEEE Trans. Nucl. Sci., vol. 48(6), 2069-2073, 2001

[13] B. Brichard, A.L. Tomashuk, V.A. Bogatyrjov, A.F. Fernandez, S.N. Klyamkin, S. Girard, F. Berghmans, "Reduction of the radiation-induced absorption in hydrogenated pure silica core fibres irradiated in situ with γ-rays," J of Non-Crystalyne Solids, vol. 353, n. 5-7, pp 466-472, 2007.

[14] N. Uchida, N. Uesugi, "Infrared optical loss increase in silica fibers due to hydrogen," J. Lightw. Technol., vol. 4, no. 8, Aug 1986.

[15] J. Stone, "Interactions of hydrogen and deuterium with silica optical fibers: A review," J. Lightw. Technol., vol. 5, no.5, May 1987.

[16] S. Delepine-Lesoille, et al., "France's state of the art distributed optical fibre sensors qualified for the monitoring of the French underground repository for high level and intermediate level long lived radioactive wastes," Sensors, vol 17, no 6, June 2017.

[17] K. Nagasawa, Y. Hoshi, Y. Ohki, and K. Yahagi, "Improvement of radiation resistance of pure silica core fibers by hydrogen treatment," Jpn. J. Appl. Phys., vol 24, part 1, no. 9, 1985.

[18] B. D. Evans, "The role of hydrogen as a radiation protection agent at low temperature in low-OH, pure silica optical fiber," IEEE Trans. Nucl.Sci., vol. 35, no. 6, pp. 1215–1220, Dec. 1988.

[19] B. Brichard *et al*, "Radiation assessment of hydrogen-loaded aluminium-coated pure silica core fibres for ITER plasma diagnostic applications," Fusion Eng. Des., vol. 82, pp. 2451–2455, 2007.

[20] S. Girard et al., "Overview of radiation induced point defects in silica-based optical fibers," Reviews in Physics, 2019, doi: https://doi.org/10.1016/j.revip.2019.100032

[21] O. Humbach, H. Fabian, U. Grzesik, U. Haken, and W. Heitmann, "Analysis of OH absorption bands in synthetic silica," J of Non-Crystalyne Solids, vol. 203, pp. 19-26, Aug. 1996.

[22] J. E. Shelby, "Radiation effects in hydrogen impregnated vitreous silica," *J. Appl. Phys.*, vol. 50, no. 5, pp. 3702–3706, 1979.

[23] P.J. Lemaire, "Reliability of optical fibers exposed to hyfrogen: prediction of long-term loss increases," Optical engineering, vol. 30, no. 6, June 1991.

[24] S. Delepine-Lesoille, J. Bertrand, L. Lablonde, X. Phéron, "Hydrogen influence on Brillouin and Rayleigh distributed temperature or strain sensors," Proceedings of the 22nd Intern. Conference on Optical Fibre Sensors (OFS22), Beijing, China, 15–19 Oct. 2012.

[25] P.J. Lemaire, E.A. Lindholm, "Hermetic Optical Fibres: Carbon Coated Fibres" in Specialty Optical Fibres Handbook, A. Mendez, T.F. Morse, Eds.; New York Academic: New York, NY, USA, pp. 453–490, 2007.

[26] J.L. Leray, "Contribution à l'étude des phénomènes induits par les rayonnements ionisants dans les structures à effet de champ au silicium ou à l'arséniure de gallium utilisée en microélectronique," Ph.D. dissertation, Université de Paris Sud, centre d'Orsay, 1989.

[27] A. A. Witteles, "Neutron Radiation Effects on MOS Fets: Theory and Experiment," IEEE Trans. Nucl. Sci., Vol 15, Issue 66, pp. 126-132, 1968.

[28] A. Morana *et al*, "Influence of neutron and gamma-ray irradiations on *rad-hard* optical fiber," Optical Materials Express Vol. 5, Issue 4, pp. 898-911, 2015.